Supplementary information

Zi Dai [a], Jilin Zhang [b,c,∗], Xiaoya Zhao [a], Xiaoxun Liu [a], Yunyun Lei [b,c] Guixia Liu [a,∗]

[a] School of Chemistry and Environmental Engineering, Changchun University of Science and Technology, Changchun 130022, China.

[b] State Key Laboratory of Rare Earth Resource Utilization, Changchun Institute of Applied Chemistry, Chinese Academy of Sciences, Changchun 130022, P. R. China.

[c] University of Science and Technology of China, Hefei 230026, P. R. China.

Corresponding Authors:

E-mail: zjl@ciac.ac.cn (Zhang J.L.)

E-mail: liuguixia22@163.com (Liu G.X.)

1. Phosphate adsorption experiments

1.1 Effect of pH value on phosphate adsorption

The effect of pH on the adsorption capacity of MgAl-LDH@ZIF-8 was determined using an optimized intermittent adsorption experiment. The pH of 100 mg P/L of KH_2PO_4 solution was adjusted to 3-12 using 1 M HCl and 1 M NaOH solution. 20 mg of MgAl-LDH@ZIF-8 was added to 20 mL of phosphate solution with different pH, and the remaining phosphorus concentration was measured after shaking at 200 rpm at 25 ℃ for 24 h. The adsorption capacity was calculated, and the optimal pH value could be derived. The following adsorption experiments were performed at the optimal pH.

The adsorption capacity (q_e, mg/g) and removal rate (R, %) were calculated by the following equations (1) and (2) :

$$q_e = \frac{(C_0 - C_e)V}{m} \tag{1}$$

$$R = \frac{C_0 - C_e}{C_0} \times 100\% \tag{2}$$

Where q_e (mg/g) represents the adsorption capacity, R (%) is the removal rate, C_0 (mg/L) and C_e (mg/L) represent the initial concentration of phosphate solution and the residual concentration after adsorption, respectively. m (mg) is the mass of the adsorbent and V (mL) represents the volume of phosphate solution.

1.2. Adsorption kinetics

To investigate the effect of different times on the adsorption properties of phosphate, 200 mg of ZIF-8, MgAl-LDH and MgAl-LDH@ZIF-8 were dispersed in 200 mL of 100 mg P/L KH_2PO_4 solutions (pH = 6). The solution was shaken at 200 rpm for 5-2880 min, and 1 mL of the solution was removed at specific time intervals, filtered through a 0.45 μm filter membrane, and the phosphate concentration was determined.

To probe into the adsorption mechanism of phosphate adsorption by the adsorbent, the obtained data were fitted with pseudo-first-order (PFO) [1] and pseudo-second-order (PSO) [2] models were expressed in equations (3) and (4):

$$\ln(q_e - q_t) = \ln q_e - k_1 \tag{3}$$

$$\frac{t}{q_t} = \frac{1}{k_2 q_e^2} + \frac{t}{q_e} \tag{4}$$

where q_e, q_t (mg/g) denote the adsorption capacity at equilibrium and t time, respectively. k_1 and k_2 respectively represent the rate constant of PFO, PSO, and t represents the reaction time (min).

1.3. Adsorption isotherm

To investigate the effect of the initial concentration on the phosphate

adsorption performance, 20 mg of adsorbent was added to 20 mL of phosphate solutions with different concentrations (20-180 mg P/L), and the pH of the solution was adjusted to 6. After shaking at 200 rpm for 24 hours at 25 °C, it was filtered through a 0.45 μm filter and the phosphate concentration was determined. The results of the adsorption isotherms were fitted with the Langmuir model [3] (equation (5)) and the Freundlich model [4] (equation (6)).

$$\frac{C_e}{q_e} = \frac{1}{q_m K_L} + \frac{C_e}{q_m} \tag{5}$$

$$ln q_e = \frac{1}{n} ln C_e + ln K_F \tag{6}$$

Where q_m (mg/g) represents the maximum adsorption capacity, K_L (L/mg) is the Langmuir equilibrium constant, K_F ((mg/g) / (mg/L) 1/n) is the Freundlich equilibrium constant, and n is the coefficient of the Freundlich model.

1.4. Adsorption thermodynamics

To investigate the effect of different temperatures on the adsorption properties of phosphate, thermodynamic parameters at three temperatures, 298 K, 303 K, 308 K, 313 K and 318 K, were studied. The experimental steps were the same as those for the adsorption kinetics, except for the difference in temperature. The thermodynamic parameters were calculated by the following equations (7-9) [5].

$$k_c = \frac{q_e}{c_e} \tag{7}$$

$$ln k_c = \frac{\Delta S^0}{R} - \frac{\Delta H^0}{RT} \tag{8}$$

$$\Delta G^0 = \Delta H^0 - T \Delta S^0 \tag{9}$$

Where ΔH^0 (KJ/mol), ΔS^0 (KJ/mol K), and ΔG^0 (KJ/mol) represent the enthalpy change, entropy change, and Gibbs free energy respectively. Kc (L/g) denotes the thermodynamic equilibrium constant, T (K) is the adsorption temperature R (8.314 J/mol/K) is the ideal gas constant.

1.5. Effect of co-existing ions on phosphate removal

To evaluate the effect of coexisting anions on phosphate adsorption performance, $NaNO_3$, $NaCl$, Na_2CO_3, and Na_2SO_4 were weighed and added to 100 mg P/L of KH_2PO_4 solution to prepare a solution with a coexisting anion concentration of 0.1 M, respectively. The remaining phosphate concentration was measured and the adsorption capacity was calculated after 20 mg of MgAl-LDH@ZIF-8 was added to 20 mL of the solution and shaken at 200 rpm for 24 h.

1.6 Reusability of MgAl-LDH@ZIF-8

The reuse of adsorbents is important in practical applications. In this experiment, 200 mg of MgAl-LDH@ZIF-8 was dispersed in 200 mL, 100 mg P/L phosphate solution and shaken at 200 rpm for 24 h at room temperature. At the end of adsorption, the remaining phosphate concentration of the solution was measured. Then, the adsorbent was separated by filtration and eluted with 0.1 M NaOH solution. The eluted adsorbent was dried and the adsorption experiment was performed again under the same conditions.

1.7 Simulated wastewater adsorption experiment

To explore the practicality of adsorbents, simulated wastewater solutions were prepared according to the highest phosphate content (30 mg/L) in untreated wastewater reported in the literature[6]. The concentrations of other ions in the simulated wastewater are shown in Table S4. Weigh 20, 30, 40, and 50 mg of ZIF-8, MgAl-LDH, and MgAl-LDH@ZIF-8, respectively, into 20 mL of simulated wastewater solution, and shake at 200 rpm for 24 h at 25 ℃. After shaking, the remaining phosphate concentration was measured after filtration through a 0.45 μm filter.
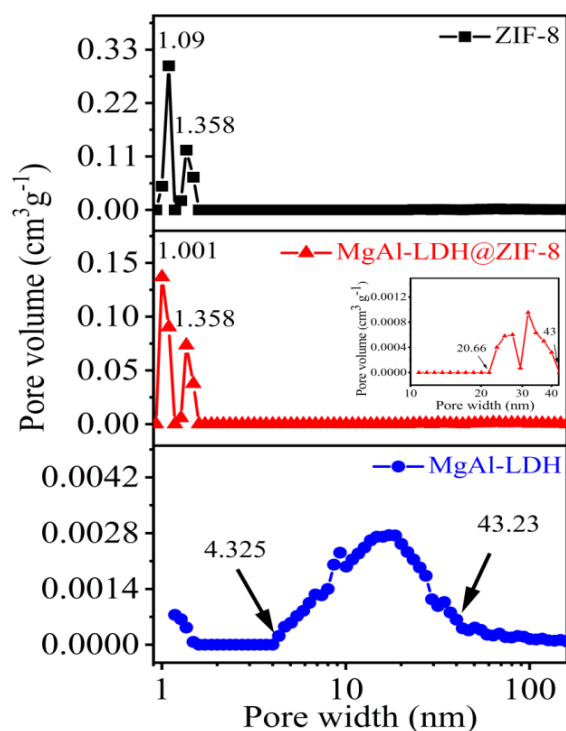
Fig. S1 Pore size distributions of ZIF-8, MgAl-LDH and MgAl-LDH@ ZIF-8.

Table S1 Surface area and pore characteristics of the samples.

Sample	S_{BET} (m^2/g)	Pore volume (cm^3/g)	pore size (nm)
ZIF-8	1659.54	0.70	1.09, 1.358
MgAl-LDH	18.40	0.06	4.325-43.23
MgAl-LDH@ZIF-8	1133.31	0.44	1.001, 1.358，20.66-43
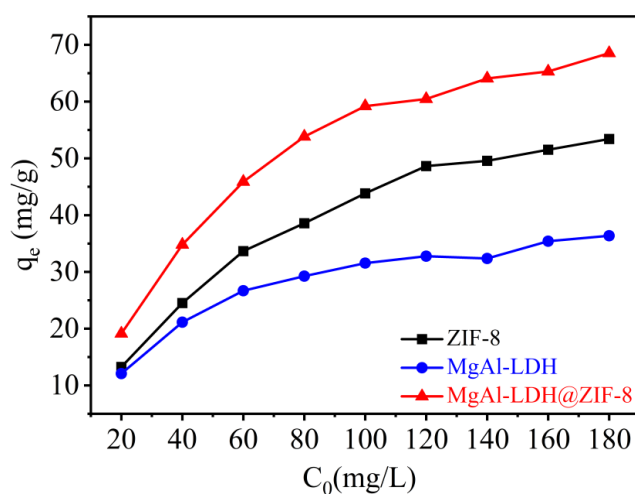
Fig. S2 Adsorption curves of ZIF-8, MgAl-LDH and MgAl-LDH@ZIF-8 at different concentrations.

Table S2 Comparison of the phosphate adsorption capacities for different adsorbents.

Adsorbent	Adsorption capacity (mg g^{-1})	Reference
MFC@UiO-66	16.95	[7]
PAN$_{T-C2-OH}$F	24.44	[8]
HA-MNP	28.9	[9]
ZrO$_2$/SiO$_2$	43.8	[10]
Zr@Fu MOF	56.41	[11]
Fe$_3$O$_4$@MgAl-LDH@La(OH)$_3$	66.5	[12]
Al-Fum	67.62	[13]
La$_5$EV	79.6	[14]
La/Fe-NB	99.46	[15]
HP-MOFs	186.6	[16]
Fe$_3$O$_4$/TiO$_2$/NH$_2$–UiO–66	192.334	[17]
MgAl-LDH	36.18	This work
ZIF-8	53.41	This work
MgAl-LDH@ZIF-8	68.53	This work

Table S3 Thermodynamic constants of phosphate adsorption by MgAl-LDH@ZIF-8

T(K)	ln(k$_c$)	ΔG^0 (KJ/mol)	ΔH^0 (KJ/mol)	ΔS^0 (KJ/(mol K))
298	0.459	-1.156		
303	0.525	-1.368		
308	0.648	-1.58	11.479	0.042
313	0.685	-1.797		
318	0.742	-2.004		
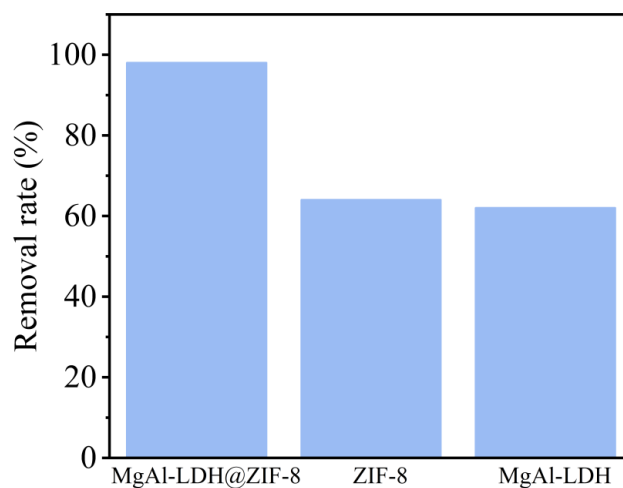
Fig. S3 Comparison of phosphate removal rates of ZIF-8, MgAl-LDH and MgAl-LDH@ ZIF-8. Conditions: phosphate concentration 30 mg/L, 20 mL; mass of adsorbent: 30 mg; time: 24 h.

Table S4.Composition of simulated wastewater used in this study

Species	Concentration (mg/L)
K^+	37.7
Na^+	74.9
Cl^-	50
SO_4^{2-}	50
NO_3^-	50
HPO_4^{2-} and $H_2PO_4^-$	30

References

[1] W. Rudzinski, W. Plazinski, Kinetics of solute adsorption at solid/aqueous interfaces: Searching for the theoretical background of the modified pseudo-first-order kinetic equation, Langmuir 24(10) (2008) 5393-5399. https://doi.org/10.1021/la8000448.

[2] A.E. Regazzoni, Adsorption kinetics at solid/aqueous solution interfaces: On the boundaries of the pseudo-second order rate equation, Colloids and Surfaces a-Physicochemical and Engineering Aspects 585 (2020). https://doi.org/10.1016/j.colsurfa.2019.124093.

[3] M. Fayazi, Facile hydrothermal synthesis of magnetic sepiolite clay for removal of Pb(II) from aqueous solutions, Analytical and Bioanalytical Chemistry Research 6(1) (2019) 125-136.

[4] J. He, W. Wang, F. Sun, W. Shi, D. Qi, K. Wang, R. Shi, F. Cui, C. Wang, X. Chen, Highly efficient phosphate scavenger based on well-dispersed La(OH)$_3$ nanorods in polyacrylonitrile nanofibers for nutrient-starvation antibacteria, Acs Nano 9(9) (2015) 9292-9302. https://doi.org/10.1021/acsnano.5b04236.

[5] Y. Yang, Y. Xie, L. Pang, M. Li, X. Song, J. Wen, H. Zhao, Preparation of reduced graphene oxide/poly(acrylamide) nanocomposite and its adsorption of Pb(II) and Methylene Blue, Langmuir 29(34) (2013) 10727-10736. https://doi.org/10.1021/la401940z.

[6] R. Keyikoglu, A. Khataee, Y. Yoon, Layered double hydroxides for removing and recovering phosphate: Recent advances and future directions, Advances in colloid and interface science 300 (2022) 102598-102598. https://doi.org/10.1016/j.cis.2021.102598.

[7] T. Liu, S. Zheng, L. Yang, Magnetic zirconium-based metal-organic frameworks for selective phosphate adsorption from water, Journal of Colloid and Interface Science 552 (2019) 134-141. https://doi.org/10.1016/j.jcis.2019.05.022.

[8] G. Xu, W. Xu, S. Tian, W. Zheng, T. Yang, Y. Wu, Q. Xiong, Y.K. Kalkhajeh, H. Gao, Enhanced phosphate removal from wastewater by recyclable fiber supported quaternary ammonium salts: Highlighting the role of surface polarity, Chemical Engineering Journal 416 (2021). https://doi.org/10.1016/j.cej.2020.127889.

[9] M. Rashid, N.T. Price, M.A. Gracia Pinilla, K.E. O'Shea, Effective removal of phosphate from aqueous solution using humic acid coated magnetite nanoparticles, Water Research 123 (2017) 353-360. https://doi.org/10.1016/j.watres.2017.06.085.

[10] X. Wang, L. Doug, Z. Li, L. Yang, J. Yu, B. Ding, Flexible Hierarchical ZrO$_2$

Nanoparticle-Embedded SiO_2 Nanofibrous Membrane as a Versatile Tool for Efficient Removal of Phosphate, Acs Applied Materials & Interfaces 8(50) (2016) 34668-34676. https://doi.org/10.1021/acsami.6b11294.

[11] I.A. Kumar, M. Naushad, T. Ahamad, N. Viswanathan, Facile fabrication of tunable porous zirconium fumarate based metal organic frameworks in the retention of nutrients from water, Environmental Science-Water Research & Technology 6(10) (2020) 2856-2870. https://doi.org/10.1039/d0ew00385a.

[12] Z. Lin, J. Chen, Magnetic Fe_3O_4@MgAl-LDH@La(OH)$_3$ composites with a hierarchical core-shell structure for phosphate removal from wastewater and inhibition of labile sedimentary phosphorus release, Chemosphere 264 (2021). https://doi.org/10.1016/j.chemosphere.2020.128551.

[13] E. Moumen, L. Bazzi, S.E. Hankari, Aluminum-fumarate based MOF: A promising environmentally friendly adsorbent for the removal of phosphate, Process Safety and Environmental Protection 160 (2022) 502-512. https://doi.org/10.1016/j.psep.2022.02.034.

[14] W.-Y. Huang, D. Li, Z.-Q. Liu, Q. Tao, Y. Zhu, J. Yang, Y.-M. Zhang, Kinetics, isotherm, thermodynamic, and adsorption mechanism studies of La(OH)$_3$-modified exfoliated vermiculites as highly efficient phosphate adsorbents, Chemical Engineering Journal 236 (2014) 191-201. https://doi.org/10.1016/j.cej.2013.09.077.

[15] Y. Lan, S. Gai, K. Cheng, J. Li, F. Yang, Lanthanum carbonate hydroxide/magnetite nanoparticles functionalized porous biochar for phosphate adsorption and recovery: Advanced capacity and mechanisms study, Environmental Research 214 (2022). https://doi.org/10.1016/j.envres.2022.113783.

[16] M. Li, Y. Liu, F. Li, C. Shen, Y.V. Kaneti, Y. Yamauchi, B. Yuliarto, B. Chen, C.-C. Wang, Defect-rich hierarchical porous UiO-66(Zr) for tunable phosphate removal, Environmental Science & Technology 55(19) (2021) 13209-13218. https://doi.org/10.1021/acs.est.1c01723.

[17] L. Yang, S. Zhang, X. Shan, C.-s. Ha, Q. An, Z. Xiao, L. Wei, S. Zhai, Multifunctional Fe_3O_4/TiO_2/NH$_2$-UiO-66 with integrated interfacial features for favorable phosphate adsorption, New Journal of Chemistry 46(29) (2022) 14091-14102. https://doi.org/10.1039/d2nj02852b.